Practical Pinch Torque Detection Algorithm for Anti-Pinch Window Control System Application

Hye-Jin Lee*, Won-Sang Ra**, Tae-Sung Yoon*** and Jin-Bae Park*

* Department of Electrical and Electronics Engineering, Yonsei University, Seoul, Korea
(Tel : +82-2-2123-2773; E-mail: pastelhj@control.yonsei.ac.kr)
**Guidance and Control Department, Agency for Defense Development, Taejon, Korea
(Tel : +82-42-821-4697; E-mail: wonsang@email.com)
***Department of Electrical Engineering, Changwon National University, Changwon, Korea
(Tel: +82-55-272-7513; E-mail: tsyoon@changwon.ac.kr)

Abstract: A practical pinch torque estimator based on the Kalman filter is proposed for low-cost anti-pinch window control systems. To obtain the accurate angular velocity from Hall-effect sensor measurements, the angular velocity calculation algorithm is executed with additional procedures for removing the measurement noises. Apart from the previous works using the angular velocity estimates and torque estimates for detecting the pinched condition, the torque rate is augmented to the system model and the proposed pinch estimator is derived by applying the steady-state Kalman filter recursion to the model. The motivation of this approach comes from the idea that the bias errors in torque estimates due to the motor parameter uncertainties can be almost eliminated by introducing the torque rate state. For detecting the pinched condition, a systematic way to determine the threshold level of the torque rate estimates is also suggested via the deterministic estimation error analysis. Simulation results are given to certify the pinch detection performance of the proposed algorithm and its robustness against the motor parameter uncertainties.

Keywords: Torque Estimation, Pinch Detection, Anti-Pinch Window Control System, Kalman Filter

1. INTRODUCTION

An anti-pinch window control system associated with a motor vehicle is intended for preventing injuries when an obstacle is carelessly pinched between the closing window and the sash of a motor vehicle. Detecting a pinched obstacle, the window is controlled to the predetermined position. Therefore, the system performance depends on the reliability of the pinch decision algorithm. The block diagram of the anti-pinch window control system is depicted in the Fig. 1. The system under consideration has a DC motor for window lift mechanism and one Hall-effect sensor mounted at the end of the motor shaft. The angular velocity of the motor shaft is calculated using the pulse train measured by the Hall-sensor and fed back into the controller [1].

The conventional methods to detect the pinched condition are generally classified into two categories: The differential type pinch estimator is based on the assumptions that the window moves with constant velocity under the unobstructed operating condition and the abrupt drop of velocity is occurred in the pinched condition [2]. However, this algorithm could be inadequate in real situations because the frictional torque of window frame has the normally varying characteristics through the full range of vehicle closure panel [3]. This pinch estimator requires small amount of computation but its performance could be degraded in the presence of measurement noises [2]. On the other hand, the absolute type pinch estimator takes advantage of the fast response time by using the changes of motor control current to compensate the pinch torque as well as the angular velocity [4-5]. It recognizes the pinched condition when the current exceeds a prescribed threshold. However, it cannot guarantee the robustness against the abnormal vibrations under the real driving conditions. Moreover, this method requires an additional current sensor to avoid false alarm [2-5], and could not be a general solution because the detection of pinch condition totally depends on the current limit determined by engineer's heuristic [2-3].

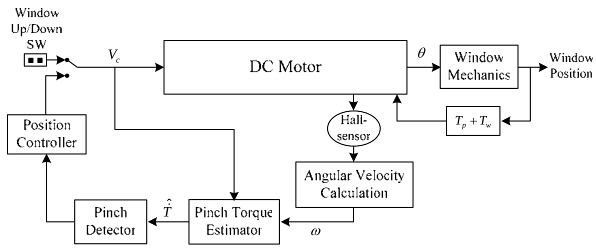

Fig. 1. Block diagram of anti-pinch window control system

In this paper, the low-cost anti-pinch window control system, which provides only the poor angular velocity measurements from Hall-sensor, is under consideration. First, to improve the quality of measurements, a new angular velocity calculation algorithm is proposed. The impulsive noise rejection algorithm is developed to make up the weak points in the conventional velocity calculation method. Then, using the angular velocity measurement, a new pinch detection algorithm based on the steady-state Kalman filter is proposed to overcome the limitations of the conventional pinch torque estimators. The vibration torque according to road conditions, the vibrations of reference voltage and the measurement noises are regarded as disturbances and modeled by white noises. Especially, to reflect the time-varying nature of the frictional torque which is proportional to window travels, an augmented motor model with the torque rate state is suggested. Since the torque rate estimate is less sensitive to the motor parameter uncertainties, the pinch detection algorithm using the torque rate can accommodate the high fidelity. In addition, by analyzing the influence of the motor parameter uncertainties on the estimation errors, a systematic way to determine the threshold level of torque rate at pinched condition is introduced. Simulation results show the pinch detection performance and robustness of the proposed method.

2. ANGULAR VELOCITY CALCULATION ALGORITHM FROM HALL-SENSOR OUTPUTS

The angular velocity of the DC motor can be calculated from output of Hall-sensor, which produces the pulse train with some noises. The output of Hall-sensor is depicted in Fig. 2. One pulse means that one of the magnets installed at the motor shaft with constant displacement is passed. In order to obtain the angular velocity accurately, the velocity calculation algorithm is able to suppress some noises if possible. The entire flow chart of the angular velocity calculation algorithm is summarized in Fig. 3. The detailed description of each step is given below;

The output voltage of Hall-sensor and the acquisition time at the measured instant are obtained and all parameters are initialized. Because the angular velocity to be computed is an input of pinch torque estimator, it is yielded at every sampling time of the estimator. Within the period of estimator, the current angular velocity is calculated by using the accumulated number of edges during the filter sampling period as

$$\omega_c = \frac{2\pi}{N_m} \cdot \frac{N_{edge}}{\Delta t} \tag{1}$$

where ω_c is a current angular velocity and Δt is the time interval between the first and final edges. N_m and N_{edge} are the number of magnets at the motor shaft and edges of Hall-sensor output, respectively. The edge number N_{edge} can be obtained by counting the crossing reference output voltage of Hall-sensor, V_{ref} .

$$\left(V_{k-1} - V_{ref}\right) \cdot \left(V_k - V_{ref}\right) < 0 \tag{2}$$

At this point, the reliability of edge counting is investigated. If only the current time interval between the most recent two edges is more than the 1/3 times of the previous interval, an edge occurrence is confirmed and the number of edge is increased.

Generally, the range of angular velocity is bounded. Hence, by considering the operation range of the motor, one should

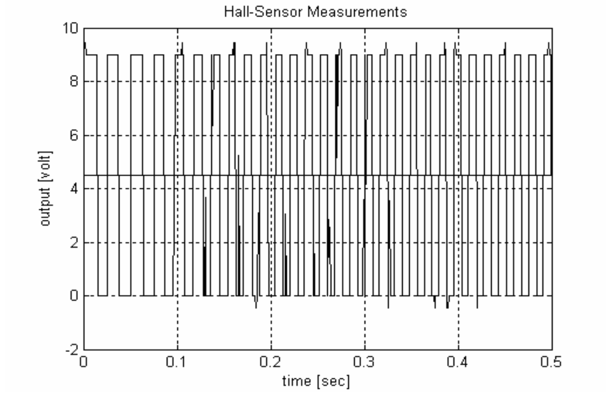

Fig. 2. Hall-effect sensor measurements

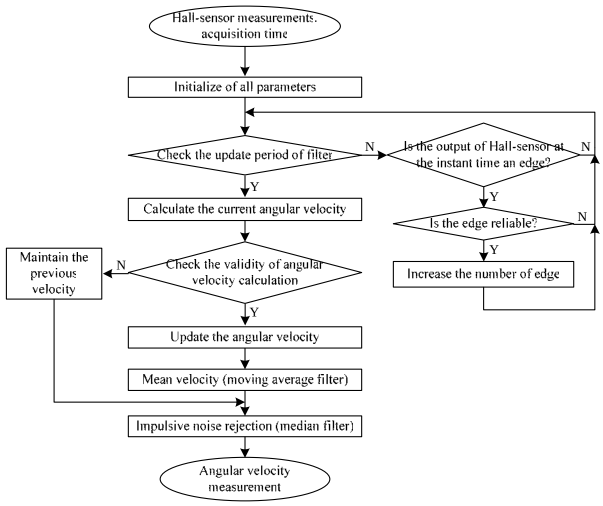

Fig. 3. Flow chart of angular velocity calculation algorithm

check whether or not the instantaneous velocity and its variation satisfy the operation ranges.

$$\left|\Delta\omega\right| \le \Delta\omega_{\max} \;\; \& \;\; \left|\omega_c\right| \le 1.1 \times \omega_{\max} \tag{3}$$

where $\Delta\omega$ is the difference between the previous and current velocity. $\Delta\omega_{\max}$, $\omega_{\max}$ are the predetermined maximum limit of velocity difference and maximum limit of velocity, respectively. If the calculated angular velocity is beyond the nominal range, it is discarded and the output velocity is maintained as the previous value.

The averaged angular velocity is obtained using the 3-point moving average filter [6]. And then, to eliminate the impulsive noises, the 7-point median filter is applied. The result passed through the two filters becomes the final output of the angular velocity calculation algorithm.

3. KALMAN FILTER BASED PINCH TORQUE ESTIMATION

3.1 State-space model for pinch torque estimator

As shown in the Fig. 4, the DC motor system to drive window can be linearized by neglecting the nonlinear characteristics such as backlash, slew-rate, coulomb friction,

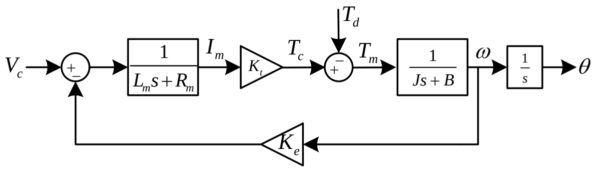

Fig. 4. Linearized motor model

etc. The nomenclature list of the linearized motor model is given below:

ω	angular velocity (speed)
θ	angular position
V_c	driving voltage (controlled voltage)
I_m	armature current
T_m	rotational torque
T_d	disturbance torque
L_m	armature inductance
R_m	armature resistance
J	moment inertia
B	viscous friction coefficient
K_e	back electomotive force (emf) coefficient
K_t	torque coefficient

The transfer function from the rotational torque of DC motor to the angular velocity in Fig. 4 is given by

$$\frac{\omega(s)}{T_m(s)} = \frac{1}{Js + B} \tag{4}$$

The rotational torque is classified into the control torque T_c, the vibration torque T_v due to the road condition, the pinch torque T_p by the obstacle and the load torque T_w by the window weight.

$$T_m = T_c - T_d = T_c - T_p - T_w - T_v \tag{5}$$

Since the vibration torque varies along the road condition, the velocity variation due to the vibration torque is assumed as zero mean white noise sequence u_v without loss of generality. From (4) and (5), the motor speed can be rewritten as

$$\dot{\omega} = -\frac{B}{J}\omega + \frac{1}{J}T_c - \frac{1}{J}(T_p + T_w) + u_v \tag{6}$$

where the variance of u_v is defined by q_v^2.

Using the fact that the electrical dynamics of the motor is generally faster than the mechanical one, the motor control torque can be approximated as follow:

$$T_c \cong \frac{K_t}{R_m}(V_c - K_e\omega) \tag{7}$$

Substituting (7) for (6) yields

$$\dot{\omega} = -\left(\frac{B}{J} + \frac{K_t K_e}{JR_m}\right)\omega - \frac{1}{J}(T_p + T_w) + u_v + \frac{K_t}{JR_m}V_c \tag{8}$$

The magnitude of window load torque T_w is proportional to the window position. On the contrary, the pinch torque T_p

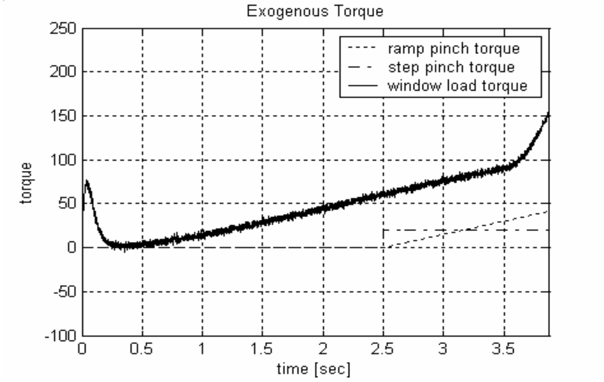

Fig. 5. Pinch torque and window load torque

appears abruptly at the pinched moment and the pinch torque profile can be changed by the type of pinched obstacles. The typical window load and pinch torque are shown in Fig. 5. Unfortunately, since the magnitude of the pinch torque is smaller than the window load torque at the end of window aperture, it is very difficult to characterize the nature of the exogenous torque using the angular velocity measurement only. Therefore, it is more effective to model these torques as a single state variable for the pinch estimator design.

$$T = T_p + T_w \tag{9}$$

The exogenous torque (9) which is closely related to the pinched condition is considered as a deterministic input to be estimated. As shown in Fig. 5, both of exogenous torques T_w and T_p, could be approximated as ramp functions with proper slopes. In this case, one of simplest ways to detect the pinch condition is to monitor the slope of exogenous torque T. Since the motor parametric uncertainty causes the bias error in the filtered torque estimate [4], the previous results using the torque estimate only is not suitable to the practical applications. To solve the problem, the torque rate $\dot{T}$ is augmented as an additional state and modeled as the random walk.

$$\ddot{T} = u_{Td} \tag{10}$$

where u_{Td} is zero mean white noise with the variance q_{Td}^2. Now, from (8), (9) and (10), one can have the state-space model for the design of pinch estimator.

$$\begin{aligned} \dot{x} &= Fx + G_c V_c + G u_c \\ y &= Hx + v \end{aligned} \tag{11}$$

where

$$x = \begin{bmatrix} \omega & T & \dot{T} \end{bmatrix}^T, \quad u_c = \begin{bmatrix} u_v & u_{Td} \end{bmatrix}^T$$

and

$$F = \begin{bmatrix} -\left(\frac{B}{J} + \frac{K_t K_e}{JR_m}\right) & -\frac{1}{J} & 0 \\ 0 & 0 & 1 \\ 0 & 0 & 0 \end{bmatrix}, \quad G_c = \begin{bmatrix} \frac{K_t}{JR_m} \\ 0 \\ 0 \end{bmatrix}, \quad G = \begin{bmatrix} 1 & 0 \\ 0 & 0 \\ 0 & 1 \end{bmatrix}$$

The covariance matrices of the process and measurement noises u_c and v are given by

$$\mathrm{cov}\langle u_c, u_c\rangle = Q = \begin{bmatrix} q_v^2 & 0 \\ 0 & q_{Td}^2 \end{bmatrix}, \quad \mathrm{cov}\langle v, v\rangle = R$$

3.2 Pinch estimator using the Kalman filter

Applying the state transition equation to the continuous system model (11), one gets the discrete-time state-space equation of the form.

$$\begin{aligned} x_{k+1} &= \Phi x_k + \Gamma V_c + u_k \\ y_k &= H x_k + v_k \end{aligned} \tag{12}$$

where the matrices are defined by using the sampling time of the filter T_s. In the proceeding filter model (12), the fluctuation of driving voltage is neglected and the voltage input is assumed as constant without loss of generality. Then the pinch estimator can be designed by applying the discrete Kalman filter recursion to the system equation (12).

$$\begin{aligned} &\hat{x}_k = \Phi\hat{x}_{k-1} + \Gamma V_c + K_{f,k}(y_k - H\Phi\hat{x}_{k-1}) \\ &K_{f,k} = P_k H_k^T R_{e,k}^{-1},\ \ R_{e,k}^{-1} = H P_k H^T + R \\ &P_{k+1} = \Phi P_k \Phi^T - \Phi P_k H^T R_{e,k}^{-1} H P_k \Phi^T + Q_d \end{aligned} \tag{13}$$

where $K_{f,k}$ is the Kalman filter gain and P_k is *a priori* estimation error covariance matrix.

Taking into account the real-time implementation issue, the steady-state Kalman filter gain is used.

$$K_f = P_\infty H^T (H P_\infty H^T + R)^{-1} \tag{14}$$

where the error covariance matrix P_∞ at steady-state holds the following discrete-time algebraic Riccati equation.

$$0 = \Phi P_\infty \Phi^T - P_\infty - \Phi P_\infty H^T (H P_\infty H^T + R)^{-1} H P_\infty \Phi + \Gamma Q \Gamma^T$$

4. DECISION OF PINCH CONDITION

4.1 Steady-state estimation error analysis

In this section, the estimation error due to the parameter uncertainties in the motor model is analyzed. The results give us new insight into the validity of the torque rate estimates for pinch detection. The uncertainties of motor parameters are able to generate the biased torque estimates. To facilitate the error analysis, the noise sources are neglected and the steady-state Kalman filter for the continuous time motor system (11) is considered.

$$\dot{\hat{x}} = (\bar{F} - K_f H)\hat{x} + K_f \omega + \bar{G}_c V_c \tag{15}$$

where

$$\bar{F} = \begin{bmatrix} -\dfrac{\bar{B}}{\bar{J}} - \dfrac{\bar{K}_t \bar{K}_e}{\bar{J}\,\bar{R}_m} & -\dfrac{1}{\bar{J}} & 0 \\ 0 & 0 & 1 \\ 0 & 0 & 0 \end{bmatrix}, \bar{G}_c = \begin{bmatrix} \dfrac{\bar{K}_t}{\bar{J}\,\bar{R}_m} \\ 0 \\ 0 \end{bmatrix}, K_f = \begin{bmatrix} K_\omega \\ K_T \\ K_{\dot{T}} \end{bmatrix}^T$$

In the above equation, $\bar{X}$ means the uncertain matrix corresponding to the nominal matrix X. From (8) and (15), the estimation error system can be obtained as the augmented state equations,

$$\begin{aligned} &\dot{z} = Az + B_c u_c \\ &e_{\dot{T}} = \dot{T} - \hat{\dot{T}} = \dot{T} - Cz \end{aligned} \tag{16}$$

where

$$A = \begin{bmatrix} -\dfrac{B}{J} - \dfrac{K_t K_e}{J R_m} & 0 & 0 & 0 \\ K_\omega & -\dfrac{\bar{B}}{\bar{J}} - \dfrac{\bar{K}_t \bar{K}_e}{\bar{J}\,\bar{R}_m} - K_\omega & -\dfrac{1}{\bar{J}} & 0 \\ K_T & -K_T & 0 & 1 \\ K_{\dot{T}} & -K_{\dot{T}} & 0 & 0 \end{bmatrix},$$

$$B_c = \begin{bmatrix} \dfrac{K_t}{J R_m} & -\dfrac{1}{J} \\ \dfrac{\bar{K}_t}{\bar{J}\,\bar{R}_m} & 0 \\ 0 & 0 \\ 0 & 0 \end{bmatrix}, z = \begin{bmatrix} \omega \\ \hat{\omega} \\ \hat{T} \\ \hat{\dot{T}} \end{bmatrix}, u_c = \begin{bmatrix} V_c \\ T \end{bmatrix}, C = \begin{bmatrix} 0 \\ 0 \\ 0 \\ 1 \end{bmatrix}^T$$

The driving voltage is assumed as step input. The window load torque and pinch torque are regarded as the ramp inputs for calculating the torque rate estimation error, since the step inputs result in the zero steady-state estimation error. On the other hand, they are considered as the step inputs to obtain the steady-state torque estimation error because the ramp inputs make the error diverge. Then, according to the final value theorem, the steady-state estimation errors can be readily derived.

$$e_{\dot{T}}(\infty) = \left(1 - \frac{\bar{R}_m(K_t K_e + R_m B)}{R_m(\bar{K}_t \bar{K}_e + \bar{R}_m \bar{B})}\right)(a_w^r + a_p^r) \tag{17}$$

$$\begin{aligned} e_T(\infty) = &\left(1 - \frac{\bar{R}_m(K_t K_e + R_m B)}{R_m(\bar{K}_t \bar{K}_e + \bar{R}_m \bar{B})}\right)(a_w^s + a_p^s) \\ &+ \left(\frac{K_t}{R_m} - \frac{\bar{K}_t(K_t K_e + R_m B)}{R_m(\bar{K}_t \bar{K}_e + \bar{R}_m \bar{B})}\right) v_c \end{aligned} \tag{18}$$

where v_c is the magnitude of motor driving voltage, and t_p is the pinched moment. a_w^r, a_p^r are the slopes of the ramp inputs and a_w^s, a_p^s are the magnitude of the step inputs for the window and pinch torque, respectively.

4.2 Decision of the threshold level

From (17) and (18), it is obvious that parametric uncertainties directly affect to the torque and torque rate estimates. However, it causes larger bias errors to the torque estimates than the torque rate estimates as shown in Fig. 9. Thus, it is better choice to use the torque rate estimate in the pinch detection algorithm. Now, the remaining problem in the development of pinch detection algorithm is to establish the systematic manner for determining the prescribed threshold level of the torque rate estimates. Before the filter converges,

$t < t_s$, the initial threshold level is determined as the maximum slope of detectable disturbance torque specified in the industrial standards. After the filter converges, $t > t_s$, the threshold level is redefined from the result of steady-state estimation error analysis using the current torque rate estimate. In general, the DC motor manufacturer maintains the parameter variations within ±10% of the nominal values. From this fact, the boundary of torque rate estimate can be obtained from (17),

$$0.74 \cdot \dot{T} \le \hat{\dot{T}} \le 1.36 \cdot \dot{T} \ , \qquad \dot{T} \ge 0 \tag{19}$$

Roughly speaking, (19) means that the reasonable threshold value to detect the pinched condition is determined as 74% of the average slope of detectable disturbance torque. That is, the resultant threshold level is set by

$$\hat{\dot{T}} \ge \hat{\dot{T}}(t_s) + \min\left(\left\|\dot{T}_p\right\|\right) \cdot 0.74 \tag{20}$$

5. SIMULATION RESULTS

The performance of the steady-state Kalman filter based pinch detection algorithm has been tested by simulation on a DC motor which has the parameters in Table 1. In the simulation, it is assumed that the measurement update time is 0.025 second and an obstacle is appeared at 2.5 second after window lifting. The exogenous torque profiles depicted in Fig. 5 are also applied. Fig. 6 shows the estimation results of the proposed pinch estimator for a step pinch torque under the nominal condition. The estimated speed, torque and torque rate abruptly change at the pinched moment. The proposed estimator performs very well even in the presence of ramp type pinch torque as in the Fig. 7. In nominal cases, the conventional disturbance torque estimator using the angular position and velocity measurements also provides good estimation performances similar to the proposed scheme [1], [5], [8]. Fig. 8 (a) indicates the simulation results for the previous torque estimator [1] using angular position in the nominal case. The performance comparison between the previous method [1] and the proposed scheme is done for the uncertain case. To observe the influence for the uncertain case, the uncertainty in the torque constant K_t is assumed as 10% of its nominal value. As shown in Fig. 8 (b) and Fig. 9 (a), the torque estimates of both filters contain bias errors as expected in this case. These results represent that the pinch detection method based on the torque estimates only is not reliable and it may provide incorrect pinch alarm. At this point, it is worth noting that the torque rate estimates of the proposed filter are free from bias error and always exceed the predetermined threshold level for deciding the pinched condition in Fig. 9 (b). Consequently, even in the uncertain cases, the proposed algorithm shows relatively robust pinch detection performance.

Table. 1 Nominal values of the motor parameters

motor parameter		value
armature inductance	L_m	3.1×10^{-3} [H]
armature resistance	R_m	3.53 [Ω]
torque constant	K_t	60 [N·m/A]
back EMF constant	K_e	0.0192 [V/(rad/sec)]
viscous friction coef.	B	2.46 [kg·m²/sec]
motor intertia	J	1.2634×10^{-2} [kg·m²]
driving voltage	V_c	12 [V]

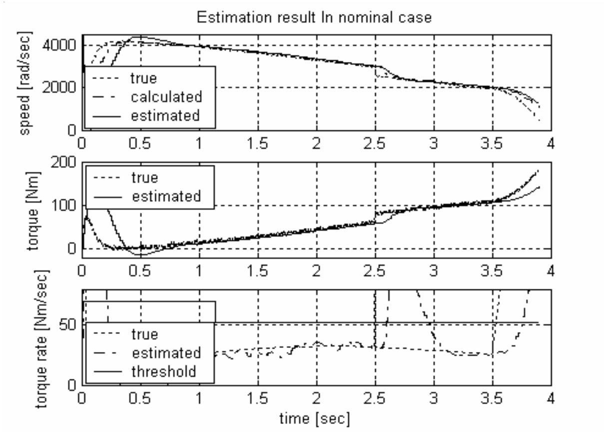

Fig. 6. Estimation result for a step pinch torque

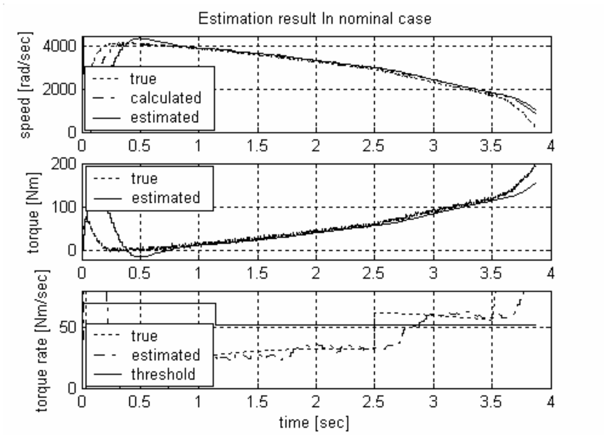

Fig. 7. Estimation result for a ramp pinch torque

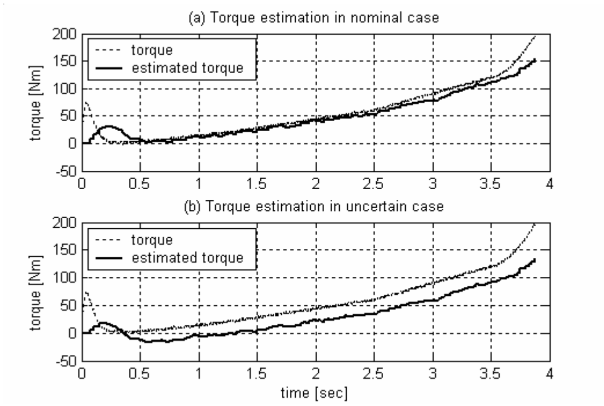

Fig. 8. Estimation result for the previous torque estimator [1]

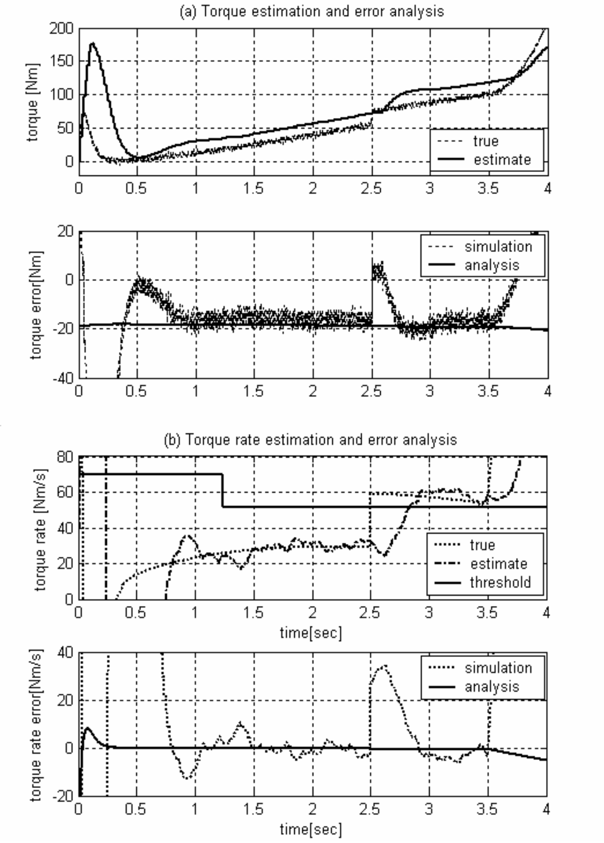

Fig. 9. Estimation result and error analysis in uncertain case

6. CONCLUSION

In this paper, the pinch torque detection algorithm based on the Kalman filter has been proposed. The angular velocity as output of Hall-sensor and measurement for the filter could be accurately calculated by involving the new methods for the noise elimination. Moreover, by considering the torque rate as an additional state variable, the proposed algorithm could improve the reliability for the pinch detection even in the presence of the parameter uncertainties. Our approach was motivated from the observation that the previous methods using the angular velocity or torque estimate often provides false pinch alarm. In addition, the results of estimation error analysis were given to derive the threshold level of torque rate estimates at pinched condition. Therefore, it can be said that the proposed scheme gives the systematic way to solve the pinch detection problem. The proposed algorithm is preferred for real-time implementation by using the steady-state Kalman filter gain. Simulation results have shown that the proposed algorithm guarantees the robust pinch detection performances. Thus, it will be a practical solution for the design of low-cost anti-pinch window control system.

REFERENCES

[1] H. W. Kim and S. K. Sul, "A New Motor Speed Estimator Using Kalman Filter in Low-Speed Range", *IEEE Trans. Ind. Electron.*, Vol. 43, No. 4, pp. 498-504, 1996.

[2] Robert P. Gerbetz, "Method of Compensating for Abrupt Load Changes in an Anti-Pinch Window Control System", *US Patent*, US2002/0190680 A1, 2002.

[3] X. de Frutos, "Anti-Pinch Window Drive Circuit", *US Patent*, US2003/0137265 A1, 2003.

[4] G. S. Buja, R. Menis and M. I. Valla, "Disturbance Torque Estimation in a Sensorless DC Drive", *IEEE Trans. Ind. Electron.*, Vol. 42, No. 4, pp. 351-357, 1995.

[5] N. Syed-Ahmad and F. M. Wells, "Torque Estimation and Compensation for Speed Control of A DC Motor Using an Adaptive Approach", *Proc. of the 36th MWSCAS*, Vol. 1, pp. 68-71, 1993.

[6] V. Lyandres and S. Briskin, "On Some Efficient Algorithm for Moving-Average Filtering", *Proc. of the 35th MWSCAS*, Vol. 1, pp. 616-619, 1992.

[7] M. Juhola, J. Katajainen and T. Raita, "Comparison of Algorithms for Standard Median Filtering", *IEEE Trans. Signal Proc.*, Vol. 39, No. 1, pp. 204-208, 1991.

[8] L. Salvatore and S. Stasi, "LKF Based Robust Control of Electrical Servodrives", *IEE Proc.-Electr. Power Appl.*, Vol. 142, No. 3, pp. 161-168, 1995.